

# 1

## The environment that conditions the Mandovi and Zuari estuaries

**S. R. Shetye, D. Shankar, S. Neetu, K. Suprit,  
G. S. Michael, and P. Chandramohan\***

*National Institute of Oceanography, Dona Paula, Goa 403 004, India.*

*\*Indomer Coastal Hydraulics (P) Ltd., Vadapalani, Chennai 600 026, India.*

---

### 1.1 INTRODUCTION

The Deccan plateau, which makes up the greater part of the Indian Peninsula, extends approximately from 10°N to 20°N. As noted by Wadia (1975), the plateau is a central tableland, with an average elevation of 600m above sea level, and is surrounded on all sides by hill ranges. To the west of the plateau and close to the western coastline of the peninsula are the Sahyadris, or Western Ghats. They extend southward from about 20°N to the Malabar Coast, where they merge into the Nilgiri Mountains (figure 1.1). South of the Palghat Gap, the Sahyadris extend through the Anaimalai Hills to the extreme south of the Indian Peninsula. The Sahyadris are called “ghats” because they are steep and terraced hills that run parallel to the coastline. The mean height of the hills is about 900m, and they are made of horizontally bedded lavas that on weathering have taken a characteristic “landing stair” shape (Wadia 1975).

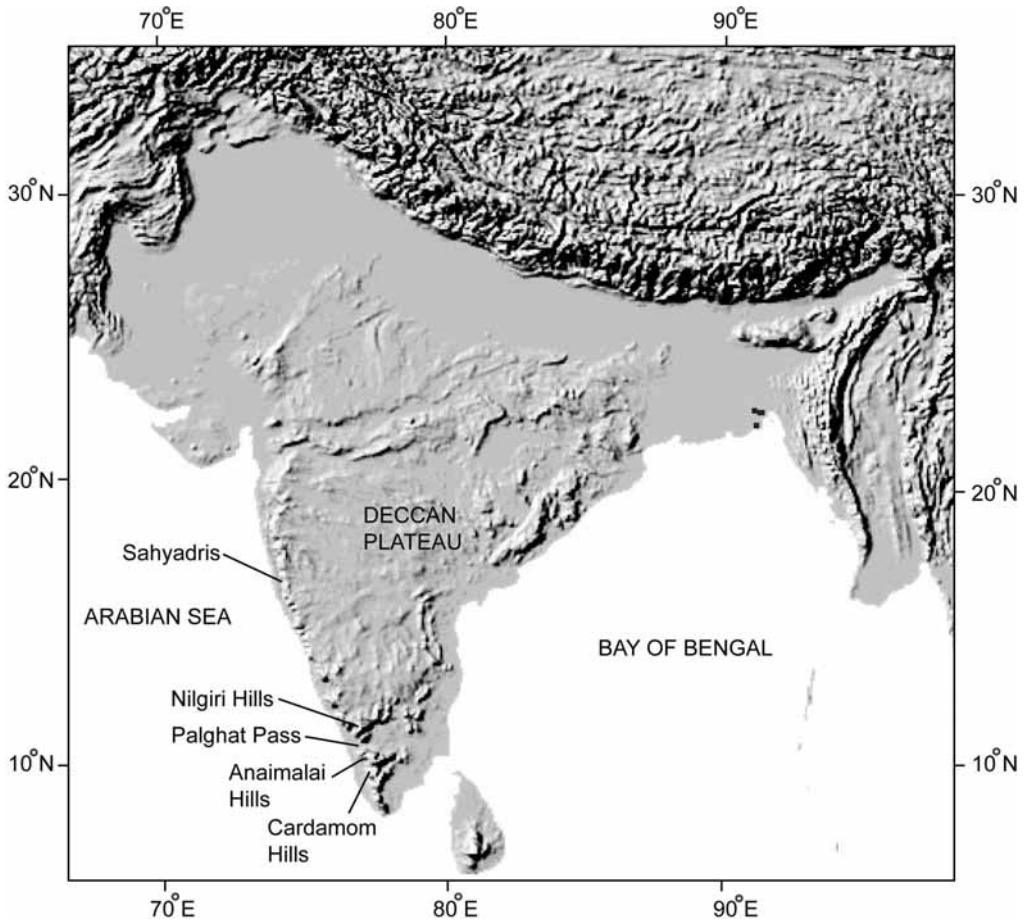


**Figure 1.1** Relief of the Indian subcontinent and its surroundings.

Between the west coast of India and the start of the rise in elevation due to the Sahyadris, there often occurs a coastal plain interspersed by small hills and other topographic features. As depicted in the schematic in figure 1.2, the typical cross-shore extent of the plain is a few tens of kilometres. With average annual rainfall in excess of 2 m, the coastal plain and the western slopes of the Sahyadris form one of the two rainiest areas of India, the other being the mountain slopes in northeastern India. Most of the rain occurs during the four months, June–September, of the Indian summer monsoon. Runoff due to the rainfall on the ridge and western slopes of the Sahyadris is carried westward down the slopes by a number of streams, rivulets, rivers, and their tributaries. The runoff is high during the four months of the monsoon, and is particularly high when the monsoon is in an active phase. After withdrawal of the monsoon, the runoff decreases rapidly, and by November reaches negligible levels.

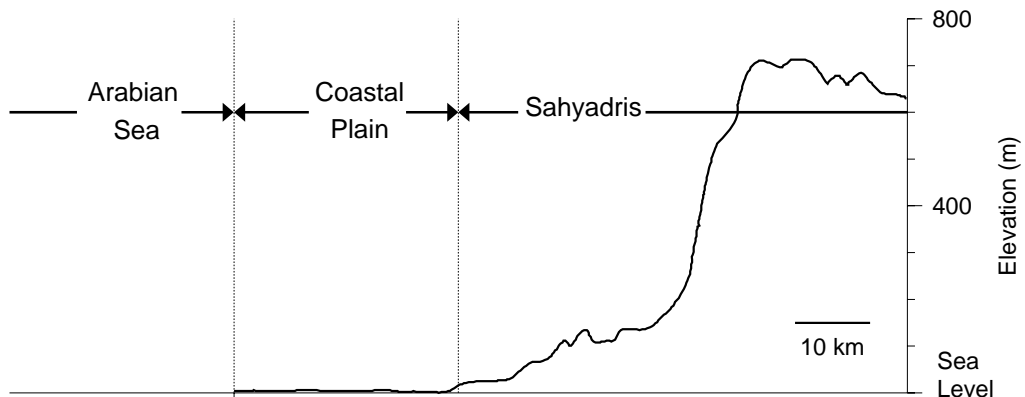


**Figure 1.2** A schematic of the typical variation in topography along the cross-shore direction on the west coast of India. Many estuarine channels that experience tides meander on the coastal plain and join the Arabian Sea. At the upstream end of these channels are rivers that arise in the Sahyadris.

The coastal plain often has estuarine networks with a main meandering channel and a number of smaller channels that are connected to it. The channels are usually of the converging kind, i.e., the width of a typical channel decreases from mouth to head. The estuarine network forms an important conduit to carry to the Arabian Sea the runoff that comes down the slopes of the Sahyadris, and that which arises from the rainfall on the plain. Hence, the freshwater content of the estuarine waters is high during the monsoon. During this season, the water level in the upstream part of the estuarine channels is controlled by the amount of runoff in the channel. The water level at the downstream end of the estuarine channel is controlled throughout the year by the astronomical tide at the coast. After withdrawal of the monsoon, the flow imposed by the tide at the mouth of the channel becomes the sole driving mechanism for transport in the estuarine network. Hence, oceanographic processes in these networks differ significantly between the wet monsoon season, when runoff is high, and the dry season, when runoff is negligible and the tide dominates circulation and mixing in the estuaries. Such estuaries are often referred to as monsoonal estuaries.

Such monsoonal estuaries occur along the entire west coast of India. They are used for dumping of domestic and industrial waste, fishing, transport of goods and people, and recreation. The banks of the estuarine channels have traditionally been preferred locations for human settlement and setting up of industries. With rapid increase in population and in industrialization during the last few decades, the estuarine channels have come under increasing stress due to anthropogenic activities. It is suspected that these activities could be causing irreversible changes in the chemistry and biology of the estuaries. As a result, issues related to the health of the estuarine networks and their ability to absorb additional impacts has gained importance. Addressing these issues requires understanding of how these estuaries

work, i.e., how the physics, chemistry, biology, and geology have in the past worked together to keep the estuary healthy, and how anthropogenic influence could be disturbing the pristine system.

The Mandovi and Zuari estuaries in the state of Goa, central west coast of India, are typical of the west coast estuaries and are also the best studied of the estuaries along the coast. This chapter describes the environment that is external to the estuaries, but influences the working of the estuaries. We begin in section 1.2 with an overview of the geometry of the channels of the estuaries. Section 1.3 examines runoff in the estuaries. Winds observed at the mouths of the estuaries are discussed in section 1.4, and waves near the mouths of the two estuaries are described in section 1.5. The chapter concludes with a discussion on special features that characterize the estuaries.

## 1.2 GEOMETRY OF THE MANDOVI AND ZUARI ESTUARINE NETWORK

Map A shows the estuarine network of the Mandovi and the Zuari. The map also shows the location up to which tides reach in the two estuaries. The Mandovi is wider, the width being approximately 4 km at the Aguada Bay. The 4 km long stretch of the bay is, on average, marginally deeper than the rest of the estuarine channel, the average depth in the bay being about 5 m. The Siquerim River joins the bay. The 6 km long stretch immediately upstream of the bay is, on average, 750 m wide and 5 m deep, i.e., the channel narrows considerably from the bay to this stretch of the estuary. The Mhapsa River joins the Mandovi at the upstream end of this stretch. Farther upstream, Diwar Island, which is approximately 11 km long, bifurcates the Mandovi into two channels. Before rejoining at the upstream end of the island, the two channels lead into an extensive network of narrow channels in a marshy area. The Cumarjua canal joins the Mandovi about 4 km upstream of Diwar Island. The 30 km stretch of the main channel of the Mandovi, from the eastern edge of Diwar Island to Ganjem, gets progressively narrower and shallower in the upstream direction. Rivers Dicholi, Valvat, Kudnem, and Khandepar join the Mandovi along this stretch. The Khandepar is the largest of the four rivers and is fed by the Dudhsagar River (not shown in Map A). At the upstream end of the Mandovi, near Ganjem, lies the Mhadei River, the major supplier of runoff to the Mandovi during the monsoon. A smaller river, Ragda, also joins the Mandovi near Ganjem. The Mhapsa River, which joins the Mandovi at Penha de France, has at its upstream end the rivers Asnoda and Moide. The Mhapsa River and its tributaries are joined by a large network of small rivulets that often flow through marshy areas.

The 10 km stretch upstream from the mouth of the Zuari, known as the Mormugao Bay, is approximately 5 km wide and 5 m deep (Map A). At the upstream end of the bay, the channel narrows to a width less than 1 km. The 30 km long channel from Cortalim to Sanvordem narrows progressively. It is less than 50 m wide at Sanvordem. The Kushavati River (also known as Paroda) joins the Zuari 4 km downstream of Sanvordem. The 10 km long stretch of the main channel from

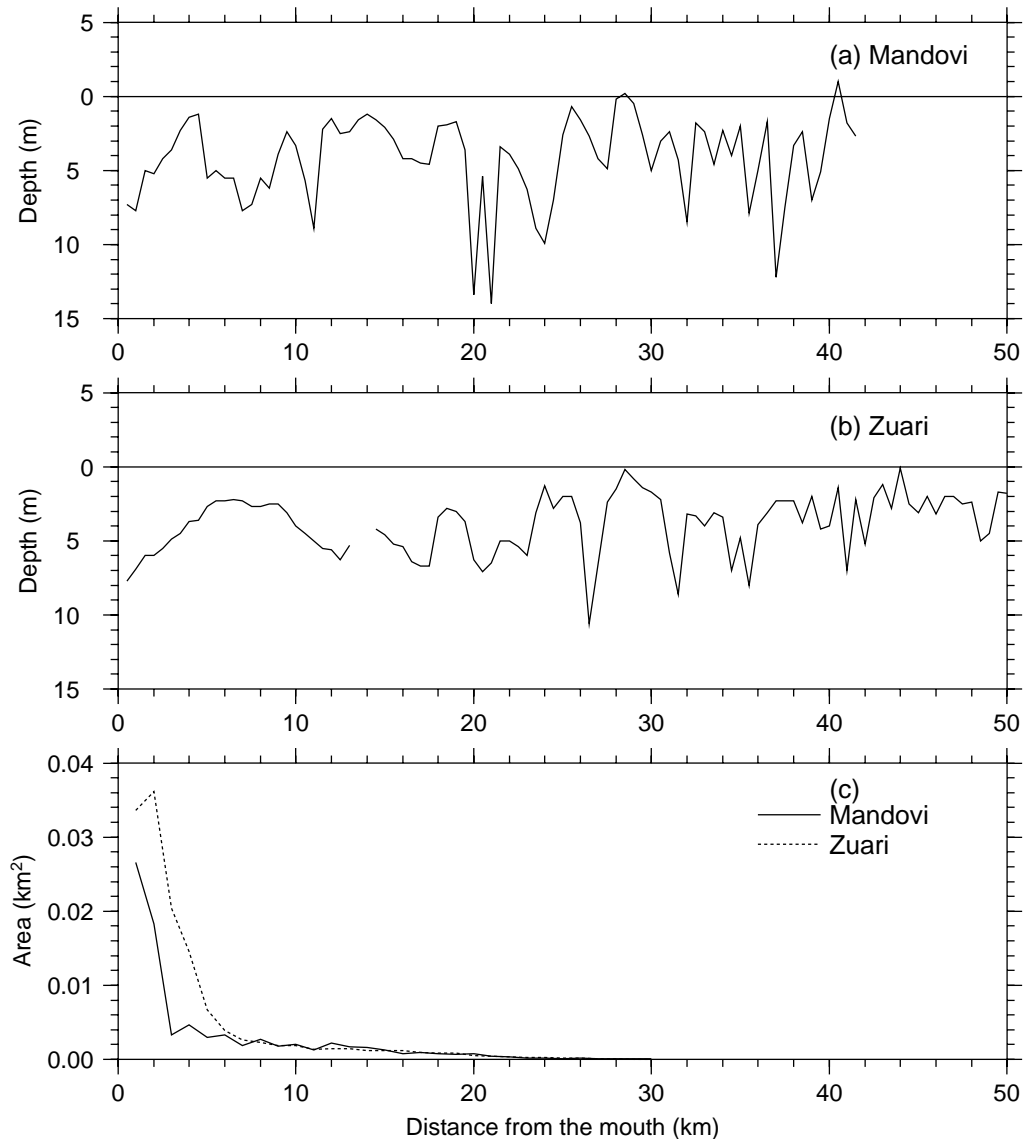


**Figure 1.3** Depth (m) with respect to mean sea level along a line in the middle of the main channel of (a) Mandovi and (b) Zuari. The horizontal scale gives distance (km) from the mouth of the two estuaries. The depth was computed by adding 1 m to the depths given in charts published by the Ministry of Shipping and Transport, Government of India. These charts are available only for those parts of the estuarine network used by iron-ore barges. Mean sea level at Mormugao is 1.3m above Spring Low Water. At the locations where depth is zero or positive, mudflats bifurcate the main channel and the flow is along the sides of the mudflats. (c) Cross-sectional area (km<sup>2</sup>), with respect to mean sea level, of the main channels of the Mandovi and Zuari. (After Shetye *et al.* 1995.)

Sanvordem to Sanguem is also known as the Sanguem River. At Sanguem, two rivers – Uguem and Guloli – join to form the Sanguem River. During the dry season, the effect of tides is felt at Sanguem, and possibly as far as 4 km upstream in the Uguem River and 1 km in the Guloli. In the Kushavati, the tidal influence is present up to about 8 km upstream of the point where it joins the Zuari. During the wet season the flow at Sanguem is dominated by river runoff.

The depth of the main channels of the Mandovi and Zuari varies considerably with location. This is brought out in figure 1.3, which shows the variation of the depth along a line in the middle of the main channels of the Mandovi and Zuari. The cross-sectional areas of the channels of the two estuaries drop rapidly in the upstream direction (figure 1.3c) primarily owing to decrease in channel width. Such channels have often been described as ‘strongly-convergent’ (Friedrichs and Aubrey 1994). The convergence has important implications for dynamics of tides in the estuarine channels.

Each of the two estuarine channels can be divided into two parts if geometry alone is considered. The first of these is distinctly wider and lies at the mouth. In the case of the Mandovi, this part is known as the Aguada Bay; Mormugao Bay is the corresponding part of the Zuari. One side of each bay is connected to the sea. The length and width of the two bays being comparable, the estuarine processes of mixing and advection here are expected to show more two-dimensional behaviour (processes along the length are as important as those perpendicular to it) than in the rest of the estuary, which in each of the two estuaries consists of a 30–40 km long converging channel. The width of the channel is well below a kilometre even at the widest end. Physical and other processes here are expected to exhibit the distinctly one-dimensional character that is commonly observed in estuaries.

### 1.3 RUNOFF

Figure 1.4 elucidates the special feature of the west coast of India that was referred to earlier: the west coast is one of the two rainiest regions of the country. This special feature is a consequence of the presence of Sahyadris: this region of high rainfall is due to orography. The moisture-laden westerlies of the summer monsoon get lifted up as they cross the Sahyadris. This leads to their cooling, and condensation of moisture and rainfall follow. The rainfall on the slopes of the Sahyadris leads to runoff in the rivers that join the Mandovi and Zuari estuaries. Virtually all of the freshwater influx into the two estuaries occurs during the summer monsoon (June–September), when most of the rainfall over the catchment area of the network occurs. The nature of temporal variability of the freshwater discharge in the main channels of the two rivers can be appreciated from the estimates of discharge (hydrographs) in the main rivers that bring freshwater to the two estuaries (figure 1.5). The monsoon season has distinct periods of high and low rainfall. These

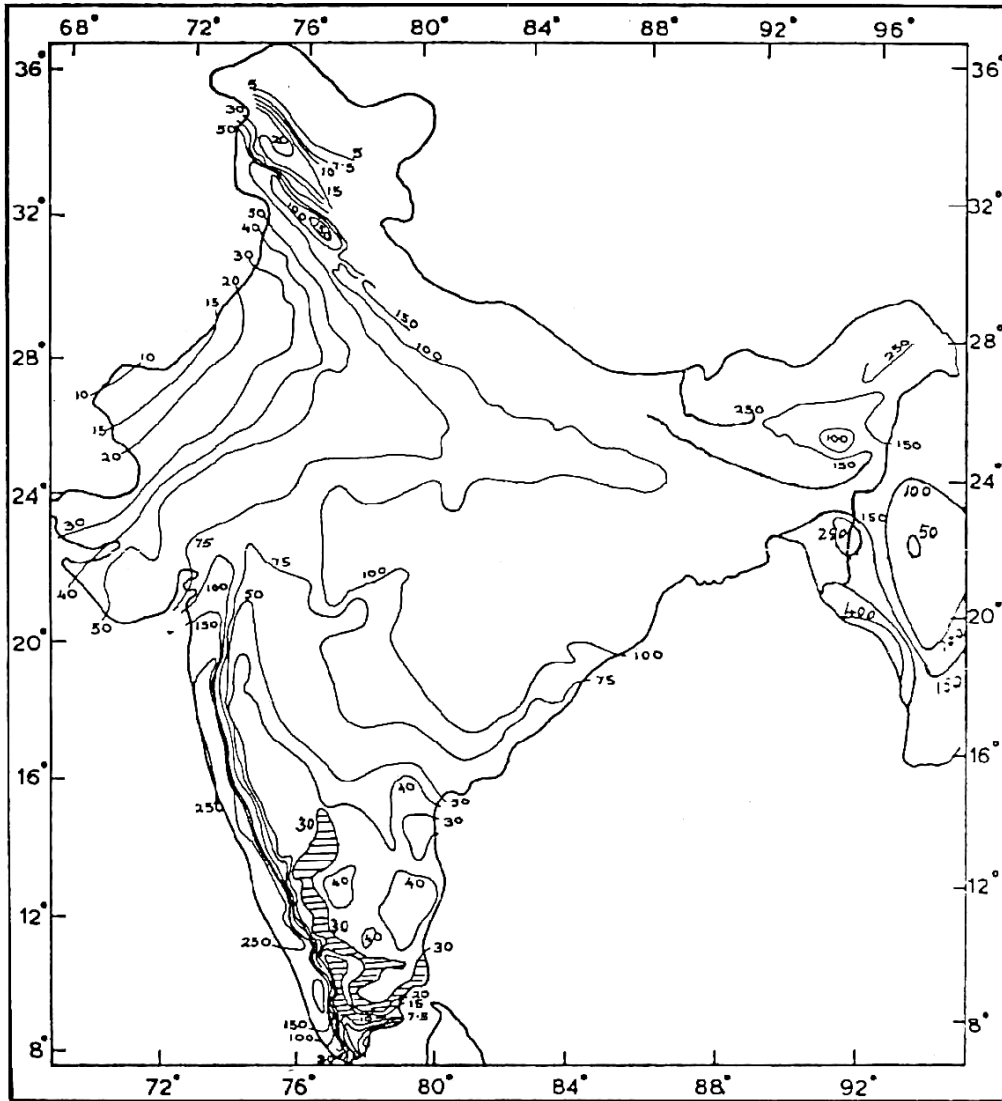


**Figure 1.4** Geographical distribution of the normal monsoon (June to September) rainfall (cm) over India. (After Rao 1976b.)

are often called active (higher than normal rainfall) and weak (lower than normal) phases of the monsoon. When a particularly active spell occurs, the entire catchment area of the Mandovi and Zuari receives copious rainfall, leading to high runoff in all the rivers. It is for this reason that some of the peaks seen in figure 1.5 occur simultaneously.

Rainfall over these basins, and hence runoff into the estuaries, being highly seasonal, the character of the estuary (salinity and nitrate, for example) varies markedly from

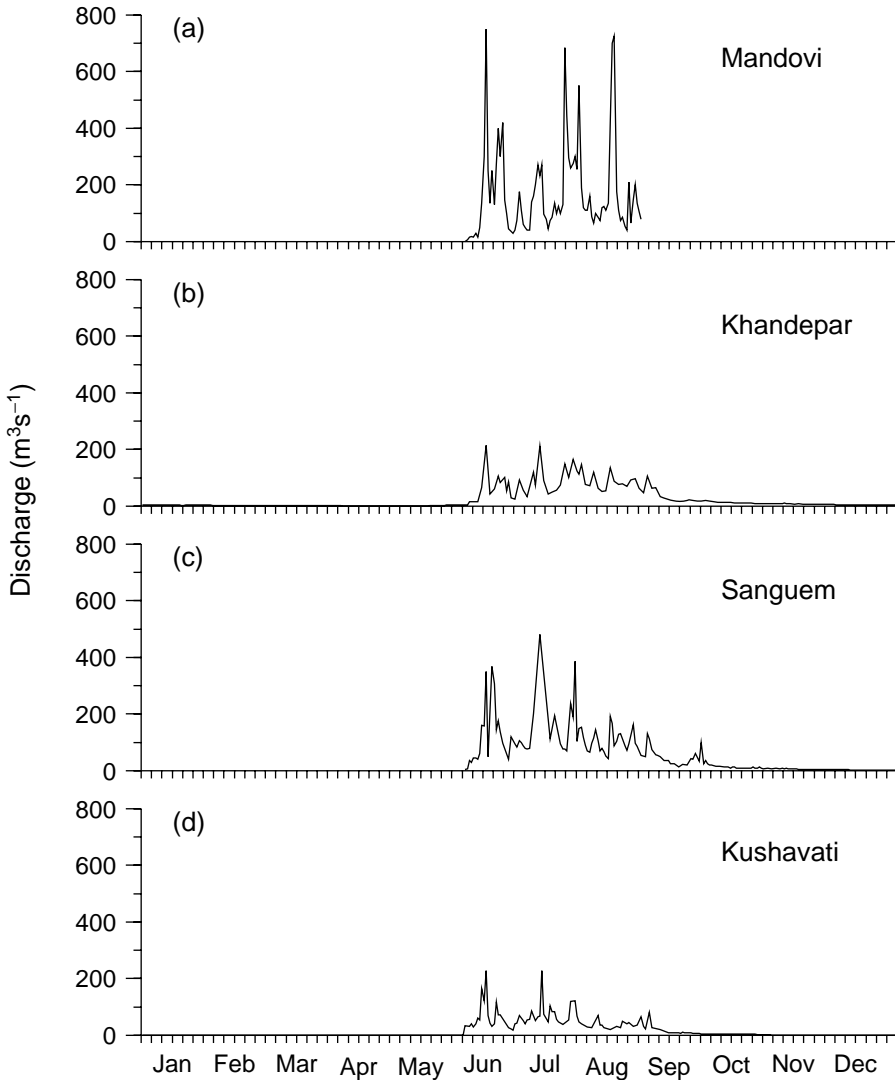


**Figure 1.5** Daily discharge ( $\text{m}^3\text{s}^{-1}$ ) hydrograph of (a) Mandovi River at Ganjem, (b) Khandepar River, (c) Sanguem River, (d) Kushavati River for 1978. Note that the discharge data for the rivers were not available for all days. The resulting 'data gaps' were removed to plot smooth curves. (This is equivalent to using linearly interpolated values for filling missing data or 'data gaps'.)

the wet to the dry season. This difference makes it important to determine the spatial and temporal variability of the runoff received by the two estuaries. Empirical data on runoff, such as that shown in figure 1.5, are too sparse to construct a comprehensive description of the runoff. Hence, we use a model to make this estimate. We begin by describing the variability of rainfall.



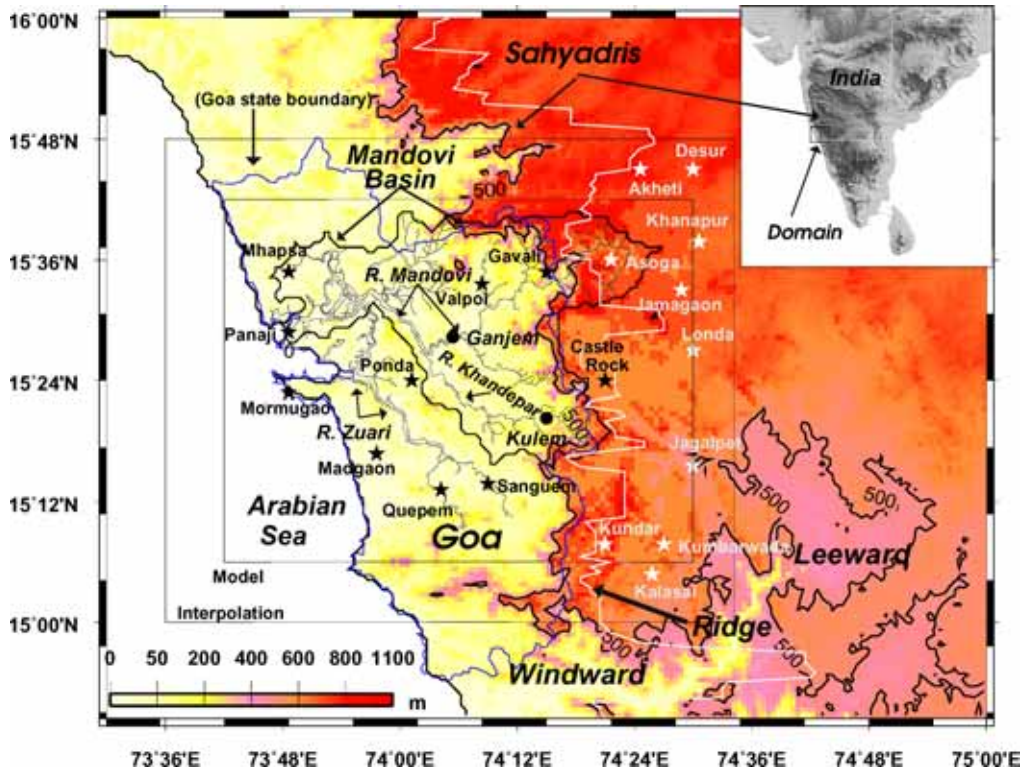


**Figure 1.6** The region of interest for rainfall interpolation and hydrological modelling. The topography of the region (along with 0 and 500m contours) as in the GLOBE (GLOBE 2004) DEM (inset topography from ETOPO2 (ETOPO2 2007)). The Mandovi and Zuari (all rivers digitized from Survey of India maps) are the two major rivers of Goa (border overlaid on the map). The Mandovi drains into the Arabian Sea near Panaji. The Mandovi basin (black curve) has two discharge gauging stations, at Ganjem on the Mhadei and at Kulem on its major tributary, the Khandepar. The outer and inner rectangles denote the interpolation and THMB model domains; rainfall interpolation was performed over a larger domain in order to include more rain gauges to map the variation. The region has two distinct topographical and climatic features: to the west lies a coastal plain with heavy rainfall (windward side), and to the east lies a plateau with less rainfall (leeward side). The white jagged line is the ridge separating the windward and leeward sides of the Sahyadris. Stations on the windward (leeward) sides are marked in black (white). (After Suprit and Shankar 2007.)

### 1.3.1 Rainfall variability

Rainfall over the Mandovi and Zuari basins (figure 1.6) varies considerably in both time and space. The seasonal cycle of rainfall, with a peak during the summer monsoon (June–September), is obvious at the rain-gauge stations in these basins (figure 1.7). There is also considerable variation of seasonal (or monthly) rainfall in space, with rainfall increasing as one proceeds from the coast towards the Sahyadris.

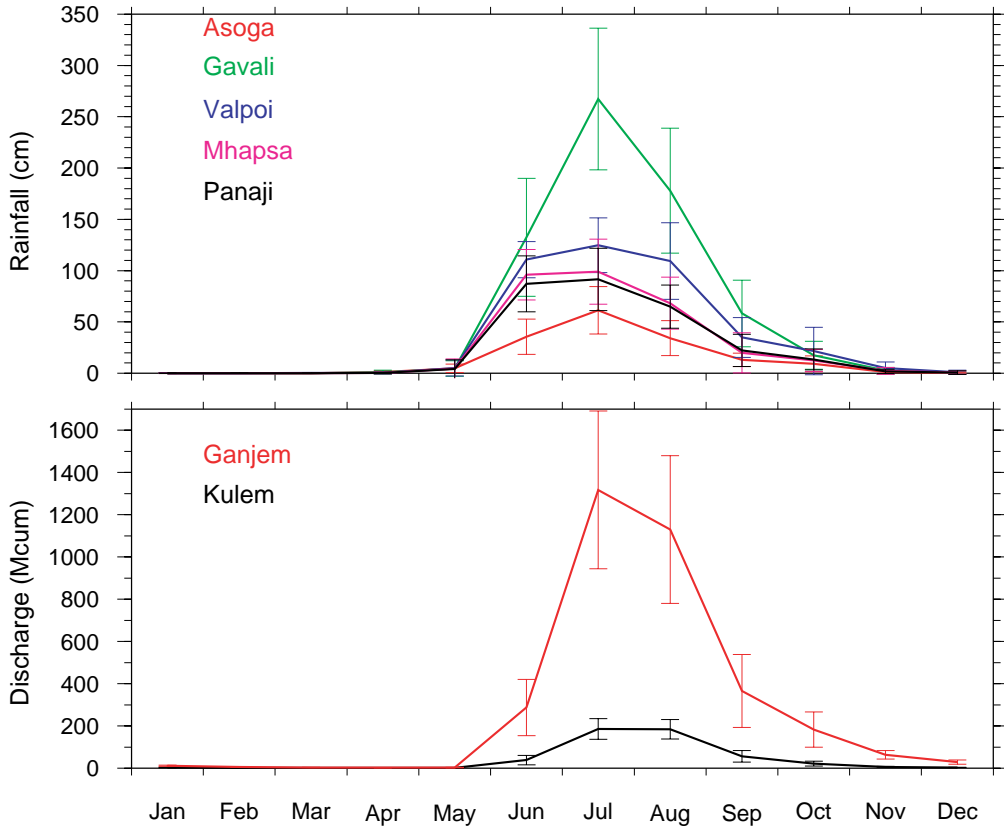


**Figure 1.7** Climatology of monthly rainfall (cm; averages computed over 1981–1997) at the five rain-gauge stations in the Mandovi basin (Panaji, Mhapsa, Valpoi, Gavali, and Asoga) and the climatology of river runoff (Mcum; averages computed over 1981–1998) at the two runoff gauging stations in the Mandovi basin (Ganjem and Kulem). The vertical bars indicate the standard deviation of the monthly rainfall and runoff; the height of the bars is a measure of the inter-annual variability.

There exist only five rain gauges in the Mandovi basin, which has an area of approximately 1895 km<sup>2</sup> (Suprit and Shankar 2007). This sparseness of rain gauges makes it difficult to map the variability in space, the problem being most acute on the slopes of the Sahyadris, where the rainfall increases rapidly as against that encountered in the flatter plains to the west, and on the leeward (eastern) side, it being difficult to capture the rapid decline in rainfall as one crosses the ghats from west to east. The annual rainfall varies from an average of 286 cm at Panaji on the coast to an average of 661 cm at Gavali on the windward slope of the Sahyadris. At Valpoi, which lies at the foothills of the Sahyadris, the average annual rainfall is 413 cm. On the leeward side, at Asoga, the average rainfall declines to 161 cm. The distance between Valpoi and Gavali and that between Gavali and Asoga is about 10 km (figure 1.6; also see the schematic in figure 1.2), showing just how rapid the spatial variation in rainfall

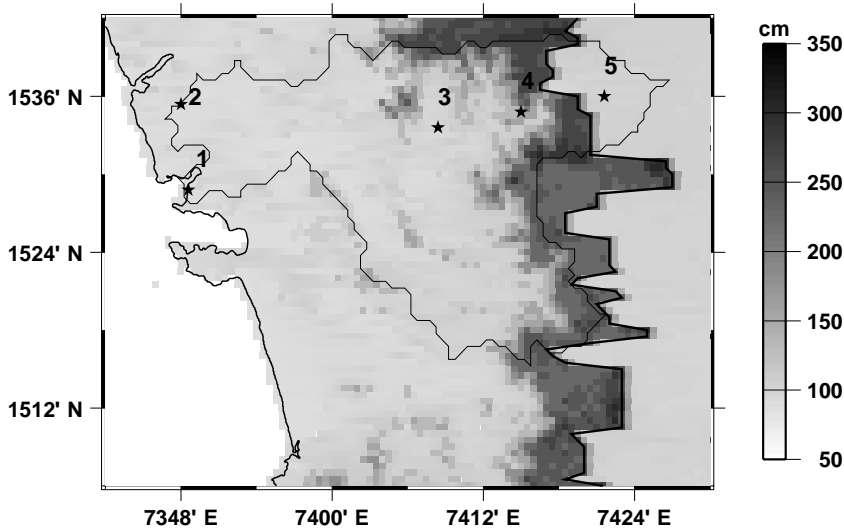


**Figure 1.8** Map of rainfall (cm) during July 1992. This rainfall map was created by interpolating the monthly rainfall separately for the windward and leeward sides and then merging the two maps. The ridge separating the windward and leeward sides is shown as the black curve. The grey curve is the Mandovi basin. The five rain-gauge stations in the basin (1–5) are the ones for which daily climatology is plotted (top–bottom in rainfall panels) in figure 1.9. (After Suprit and Shankar 2007.)

owing to the Sahyadris is. Hence, given the paucity of data to resolve this large variation in rainfall, Suprit and Shankar (2007) used a multivariate interpolation scheme that incorporated elevation as the third variable (in addition to the two horizontal co-ordinates) to map the rainfall separately for the windward and leeward sides. The ridge separating the windward and leeward sides was prescribed *a priori*. The two maps were then merged to produce a spatial map of the monthly rainfall over the region. One such map, for July 1992 (figure 1.8), shows that mapping technique captures the gradual increase in rainfall as one moves inland from the coast, the increase becoming much more rapid as one climbs the Sahyadris; the rainfall decreases rapidly on the lee side of the ghats. This picture of spatial variability of monthly rainfall is typical of the peak monsoon months of June–September, when the moisture-laden winds blow from the Arabian Sea towards the Indian west coast.

There is considerable inter-annual variability in annual rainfall (figure 1.7), the standard deviation about the mean rainfall at Panaji (286 cm), Mhapsa (303 cm), Valpoi (413 cm), Gavali (661 cm), and Asoga (161 cm) being 45, 58, 56, 173, and 50 cm respectively. This inter-annual variability in rainfall is reflected in the runoff.

There is also considerable variation in rainfall from day-to-day even during the peak monsoon months of July and August. For example, during July 1992, the total monthly rainfall at Gavali was 271 cm, but ~ 80% of this rainfall occurred over just 11 days (figure 1.9). Rainfall during the summer monsoon consists of several bursts

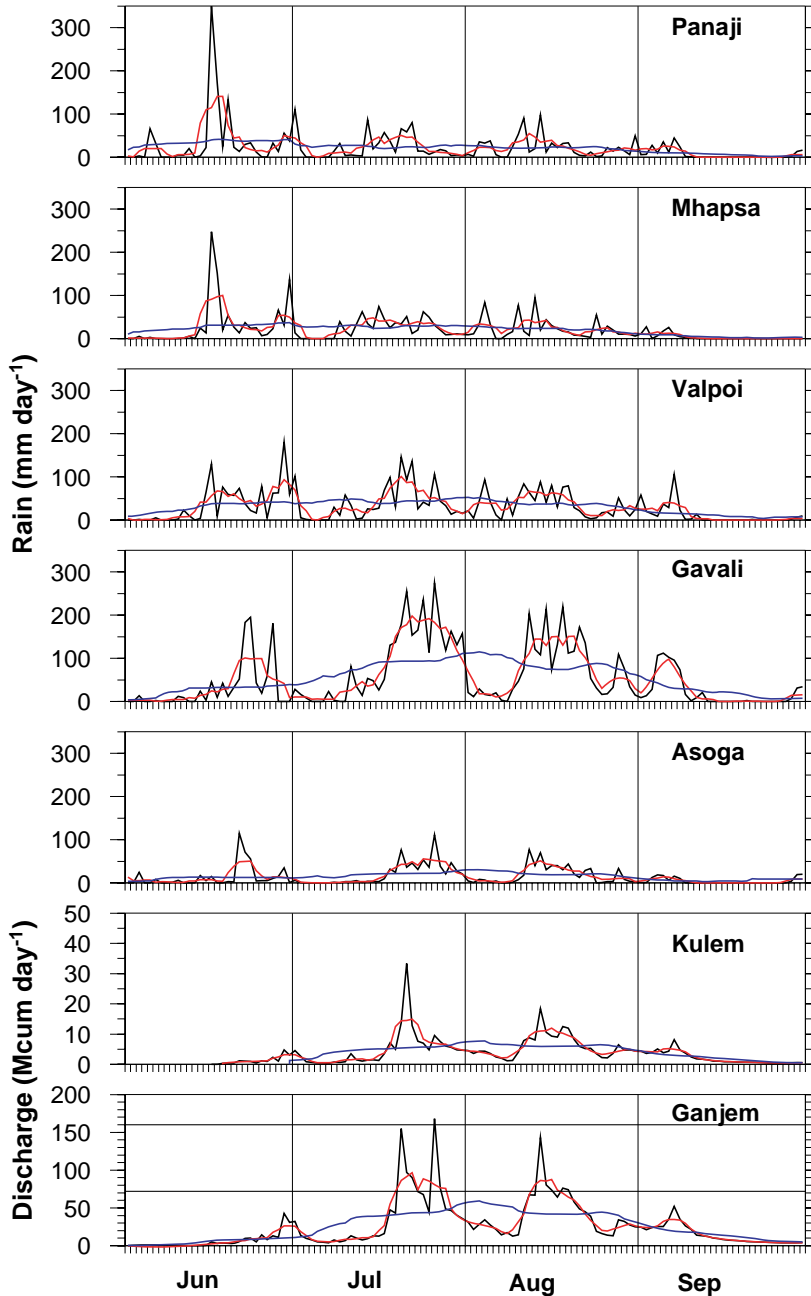


**Figure 1.9** Daily rainfall (black;  $\text{mm day}^{-1}$ ) at Panaji, Mhapsa, Valpoi, Gavali, and Asoga and daily runoff (black;  $\text{Mcum day}^{-1}$ ) at Ganjem and Kulem during June–September 1992. The horizontal line in the panels for runoff indicates the volume of the Mandovi channel. The lower line indicates the volume of the channel; alone; the upper line indicates the volume of the entire estuary, including the Aguada Bay. Overlaid on the daily rainfall and runoff are the 5-day (red) and 30-day (blue) moving averages.

during active spells of the monsoon, there being weak spells or even monsoon breaks in between them (Rao 1976b). This high-frequency variability in rainfall, evident at all rain-gauge stations, is reflected in high-frequency variability in the runoff (figure 1.9).

### 1.3.2 *The observed temporal variability of runoff in the Mandovi*

River runoff is gauged regularly at two locations in the Mandovi basin. One of them, Ganjem, is located on the Mhadei River about 50 km from the mouth of the Mandovi; the other gauging station is at Kulem, which is located on the Khandepar, the biggest of the Mandovi's tributaries (figure 1.6). The average annual runoff at Ganjem and Kulem are 3400 Mcum and 502 Mcum, the standard deviation about the mean being 648 Mcum and 91 Mcum respectively. (1 Mcum is 1 million cubic metres.)

The mean monthly runoff at the gauging stations integrates over a few rainfall bursts that result in a huge volume of freshwater being flushed through the estuarine channels within a few days. That the monsoon rainfall is characterized by bursts implies that there is considerable high-frequency variability in runoff; in other words, a large fraction of the peak runoff during July–August can be expected to occur within a few days. During 1992, for example, the daily runoff at Ganjem had a peak of 168 Mcum on 26 July (figure 1.9).

Over the rest of the year, both before and after the summer-monsoon rains, the runoff into the Mandovi is negligible. The total average runoff during November–May is 117 Mcum, much less than the 150 Mcum peaks in daily runoff (figure 1.9) during the summer monsoon.

### 1.3.3 *Spatial variability of runoff*

The gauging stations at Ganjem on the Mhadei and at Kulem on the Khandepar provide information on the amount of runoff in two of the key rivers in the Mandovi basin. The catchment area of the river at Ganjem is 872 km<sup>2</sup>, which is 46% of the Mandovi basin (Suprit and Shankar 2007). The catchment area of the Khandepar at Kulem is 97 km<sup>2</sup>, implying that the effect of rainfall over the remaining 49% of the Mandovi basin is not measured. In particular, the data available do not tell us what the runoff is at Panaji at the mouth of the Mandovi, where the estuarine channel broadens into the Aguada Bay. Hence, it is necessary to use a numerical model to make an estimate of this runoff. Shankar *et al.* (2004) assembled a framework for modelling river discharge under the sparse-data conditions prevalent in India. At the core of this framework was a hydrological model called THMB (Terrestrial Hydrologic Modelling with Biogeochemistry; Coe 2000), which, given the rainfall and evapo-transpiration at each 1 km × 1 km grid cell in the basin, routes

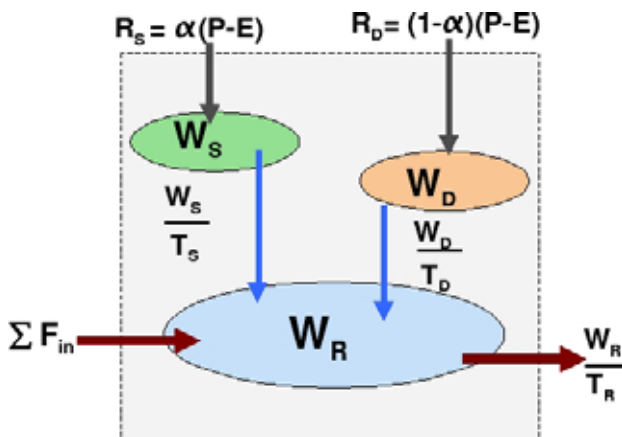


**Figure 1.10** Schematic representation of THMB. The figure shows a THMB grid cell and the fluxes into and out of the three reservoirs (surface runoff, sub-surface runoff, and river water) associated with each cell. The dashed line indicates one THMB grid cell.  $(P-E)$  denotes the runoff, the difference between rainfall and evapo-transpiration;  $\alpha$  determines the fraction of runoff (surface runoff  $R_s$ ) that goes into the surface water reservoir ( $W_s$ ),  $T_s$  being the time scale over which water flows out of the reservoir;  $R_d$  is the sub-surface runoff;  $W_d$  denotes the sub-surface water reservoir,  $T_d$  being the time scale over which water flows out of this reservoir. Water flows from both surface and sub-surface reservoirs into the river-water reservoir ( $W_R$ ), from which water flows out of the cell to a downstream cell over a timescale  $T_R$ .  $\sum F_{in}$  is the total inflow from all upstream cells into the river water reservoir.

the local grid runoff through a river channel to the sea. (This model was earlier called HYDRA: Hydrological Routing Algorithm.) In other words, THMB needs at each grid point the surface runoff, the sub-surface runoff, and the flow into it from upstream cells. Each cell, in turn, feeds into one downstream cell, thereby creating an interlocking network of cells that together constitute the model basin. (See figure 1.10 for a schematic representation of THMB.) The flow out of the cell corresponding to the gauging station is the model runoff. It is to create the rainfall forcing for THMB that Suprit and Shankar (2007) had to map the spatial variability of rainfall. Their simulated runoff matches the observed runoff at Ganjem. Hence, since the model provides an estimate of the runoff at each grid cell within the basin, it becomes a viable source of information on the spatial variability of runoff.

Note that the model river channel terminates at the point where the height falls below mean sea level in the GLOBE Digital Elevation Model (DEM) used for routing the river. For the Mandovi, this point where the river ends is in the vicinity of Panaji. The rest of the Mandovi basin, which consists of the Aguada Bay, does not form part of the river-runoff computations in THMB because the bay's bottom is below mean sea level and therefore forms part of the sea.

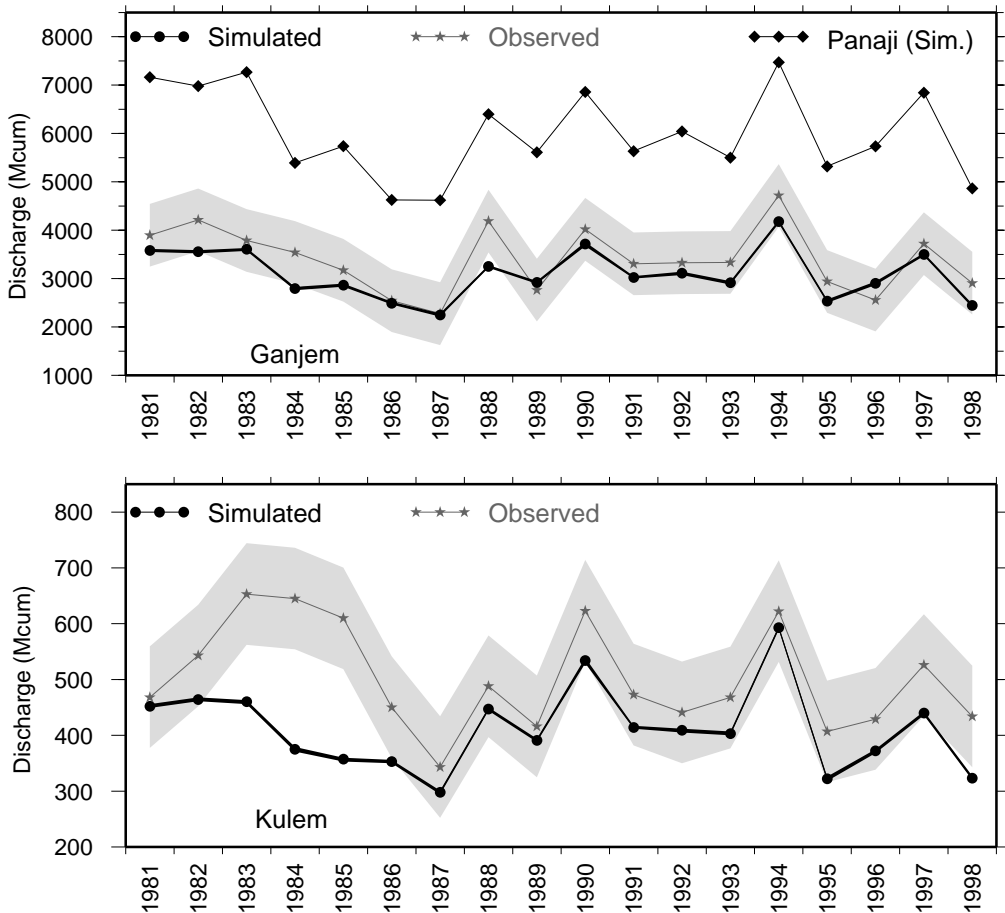


**Figure 1.11** Simulated discharges at Ganjem and Panaji (top panel) and Kulem (bottom panel). The observed discharge is plotted for comparison. The shaded area is a measure of the variability in the observed discharge; the shading is done for one standard deviation on either side of the observed discharge. The thickness of simulated discharge curves at Ganjem and Kulem show the impact of evapo-transpiration as it represents simulations obtained by reducing and increasing the evapo-transpiration by one standard deviation. Note the negligible impact of evapo-transpiration and that the error in simulated discharge is within the natural variability of the system (except in 1984 and 1988, when the black curve falls just outside the shaded region). (After Suprit and Shankar 2007.)

Runoff in the Mandovi increases almost two-fold from Ganjem to Panaji (figure 1.11) (Suprit and Shankar 2007). A large fraction of this increase comes from the tributaries Khandepar (about 45%), Valvat (about 25%; includes Dicholi and Kudnem rivers), and the Mhapsa (about 14%; includes Moide and Asnoda rivers); the balance 16% is direct flow into the estuary from the land adjoining it (figure 1.12). Note that for the reason given above, this runoff does not include that from the Sinkerim River, which flows directly into the Aguada Bay.

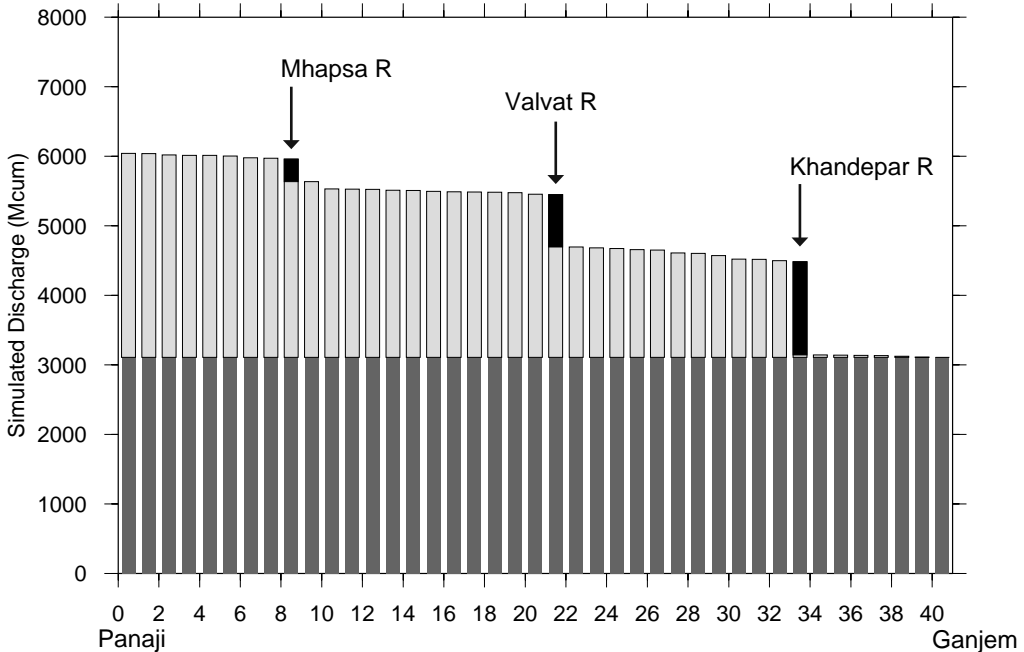


**Figure 1.12** Bar-chart showing the runoff into the Mandovi estuary from Ganjem (on the right) to Panaji (on the left) for 1992 as a function of distance (abscissa is the number of grid cells from Panaji to Ganjem) along the main channel of river. Runoff in the channel increases almost two-fold from Ganjem to Panaji, most of this increase coming from the runoff from the Khandepar, Valvat (including Dicholi and Kudnem), and Mhapsa (including Moide and Asnoda) rivers. The contributions of these tributaries are shown in black.

### 1.3.4 Runoff in the Zuari

Numerical modelling is also the only viable tool for estimating the runoff in the Zuari, there being no runoff gauging stations in this basin. Preliminary results from the numerical model of Suprit and Shankar (2007) suggest that the average (over 1981–1998) virgin (in the absence of control structures like the Selaulim Dam) annual runoff at the mouth of the Zuari near Cortalim, where it opens into the Mormugao Bay, is about 2190 Mcum. Note that the Zuari River in THMB ends at Cortalim and excludes the Mormugao Bay. The runoff just upstream of Selaulim is 491 Mcum, which matches the 75% annual dependable flow according to the observations (475 Mcum) reported in a public brochure by the Water Resources Department of the government of Goa; these measurements upstream of Selaulim were made for a few years before the dam was constructed.

### 1.3.5 Implications of dams and channel geometry to flushing

The model simulations described above do not account for control structures like dams, and estimate what is called the “virgin flow” of the river. The only functional



dam on the Mandovi is the Anjunem Dam on the Valvat or Nanda River, which joins the Mandovi downstream of Ganjem. The storage capacity of the dam is 45 Mcum, less than 1% of the runoff estimated at Panaji. Note that this dam has no impact on the runoff at Ganjem.

On the Zuari, there exists a much bigger dam, the Selaulim Dam. With a storage capacity of about 227 Mcum (about 10% of the Zuari's virgin flow at its mouth near Cortalim), this dam has a significant impact on the flow of the Zuari. The impact of such control structures is more pronounced after the summer monsoon. The error in ignoring them is comparable to the error in the observed runoff (measurement error) or the error in the simulated runoff, both of which are  $\sim 15\%$  (Suprit and Shankar 2007). After the summer monsoon, the natural runoff declines, but water is released from the dam in a controlled manner, implying a greater runoff in the dry months of January–April than would exist without the dam.

Since the model river terminates at the point where the Mandovi and Zuari estuaries widen into the Aguada and Mormugao bays, the rainfall over these bays, or the direct flow into them from other smaller rivers like the Sinquerim, is not included in the runoff estimates reported here. The rainfall over the bays, however, is expected to be mixed differently than the runoff from the main river channel flowing into it because the former represent a forcing at the surface and the latter represent a volume flux at the boundary.

The runoff in the Mandovi and Zuari estuaries is much greater than the volume of the river channel. The volume of the Mandovi (excluding the Aguada Bay) is about 70 Mcum, which is less than half the typical daily peak runoff (about 150 Mcum) at Ganjem. The daily runoff at Panaji during a summer-monsoon burst would be even greater. Hence, in an average year, the volume of freshwater flowing through the Mandovi exceeds the volume of the estuary by a factor of about 20 if using the Ganjem runoff and 40 if using the Panaji runoff. Most — over 95% — of this freshwater flux occurs during June–October, implying that the water in the river channel (till the Aguada Bay) is flushed out and renewed several times over during the summer monsoon. During the 26 July 1992 runoff burst of 168 Mcum (measured at Ganjem) (figure 1.9), the volume of freshwater flowing through the river was more than twice its volume. Note that this burst of 168 Mcum matches the 160 Mcum volume of the Mandovi when the Aguada Bay is included. Similar behaviour can be expected in the Zuari, which has a smaller volume (less than 50 Mcum) till Cortalim (matching its smaller catchment area in comparison with the Mandovi). Inclusion of the Mormugao Bay increases the volume of the Zuari to over 270 Mcum, but the runoff over a few days during July–August would still flush the Zuari completely.

Such flushing of the Mandovi and Zuari occurs during the summer monsoon every year. Physically, the implication is that the channel of the estuary is completely flushed with freshwater during just a few days of the summer monsoon. Such episodes are expected to turn the estuarine water fresh from head to mouth.

Over the rest of the year, however, such flushing does not occur over the entire channel because the runoff decreases considerably. At Ganjem on the Mandovi,

for example, the average runoff during December–May is about 18Mcum, which is much less than the estuary's volume. For some distance from the head of the estuary, however, even this meagre runoff will tend to freshen the channel (over 5–10 km), implying that salinity should decrease towards the head of the river even during the lean months.

#### 1.4 WINDS

In the Mandovi and Zuari estuaries, the impact of winds is expected to be felt primarily either through vertical mixing that waves generated on the surface would induce or through the circulation set up owing to the stress exerted by winds. Neither of these impacts has so far been shown to be significant. For example, it is not clear how the turbulence generated in the water column by tidal flow compares with that generated by winds. Nonetheless, winds form an important environmental variable for any marine system. It is important to examine the annual cycle of winds to understand the environment in which the two estuaries exist.

The winds reported here were measured (for one year during 1 June 1996 to 31 May 1997) near the mouths of the two estuaries; the measurements were made on the campus of the National Institute of Oceanography at Dona Paula (see Map A) using an anemometer located on the terrace of the main building of the institute. The anemometer was located at a height of about 50m above sea level. The recorded data were ten-minute vector averages of wind speed (figure 1.13) and direction (figure 1.14). The data show striking differences between the summer monsoon and the rest of the year. During the summer monsoon, winds are stronger and do not always exhibit the distinct diurnal variation in wind speed seen after the monsoon withdraws.

As seen in figure 1.13, on 8 June 1996 there was a distinct increase in wind speed heralding arrival of the monsoon. Panaji received the first rains of the season on that day. The maximum wind speed recorded on that day was well over twice the daily maximum speed during the first week of June. Also, the daily diurnal cycle of wind speed, with maximal wind around noon or in the afternoon, which was observed during the first week of June, was absent on 8 June. In fact, the diurnal cycle was hardly noticeable on most days from the onset of monsoon till about the middle of August. During this time there was a period, approximately from mid-June to mid-July, when the wind was consistently from one direction, from about 330 degrees, and wind speed was roughly between 4 and 7  $\text{ms}^{-1}$ . Climatological monthly-mean data generally report that winds at this time are westerly or southwesterly (see, for example, Shetye *et al.* 1985). The northwesterly or northerly angle of wind direction observed in figure 1.14 may well be a local feature arising from local terrain.

The strength of the winds decreases after the withdrawal of the summer monsoon. After the withdrawal and until the onset of the next monsoon, i.e., from October to

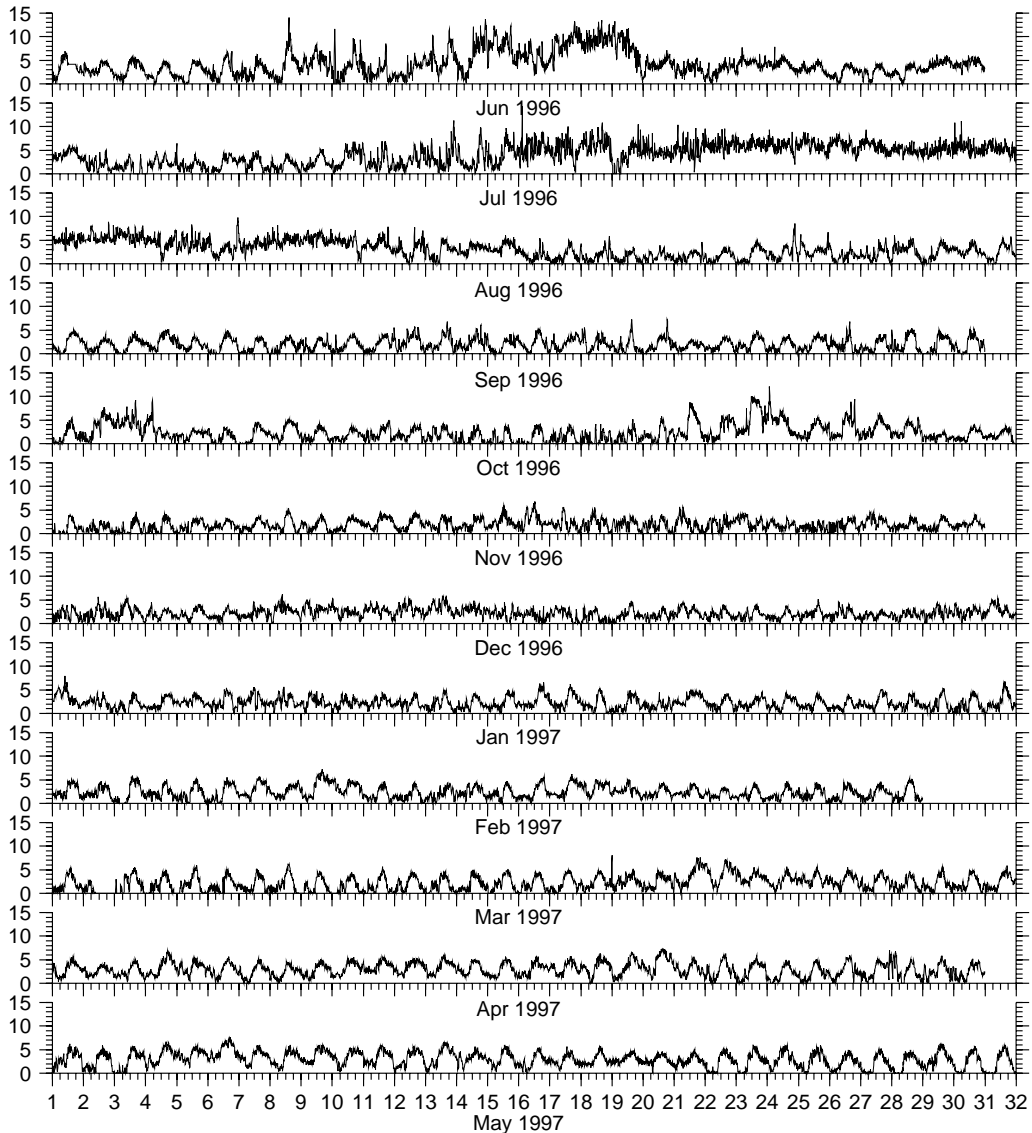


**Figure 1.13** Wind speed ( $\text{ms}^{-1}$ ) during 1 June 1996 to 31 May 1997. The horizontal axis gives date of the month shown at the bottom of each panel. Vertical axis gives wind speed.

the end of May or early June, the wind field is dominated by the sea breeze. The winds are strongest in the afternoon, when the cross-shore component is from sea towards land. During early morning, the winds are weaker and the cross-shore component is from land to sea. Though these characteristics do repeat from day to day, details differ. Figure 1.15 shows the hodograph, taken from Neetu *et al.* (2006), that gives the average daily cycle of winds observed during 1–15 April 1997. Climatological data suggest that during April the large-scale wind field in the region is weak, and

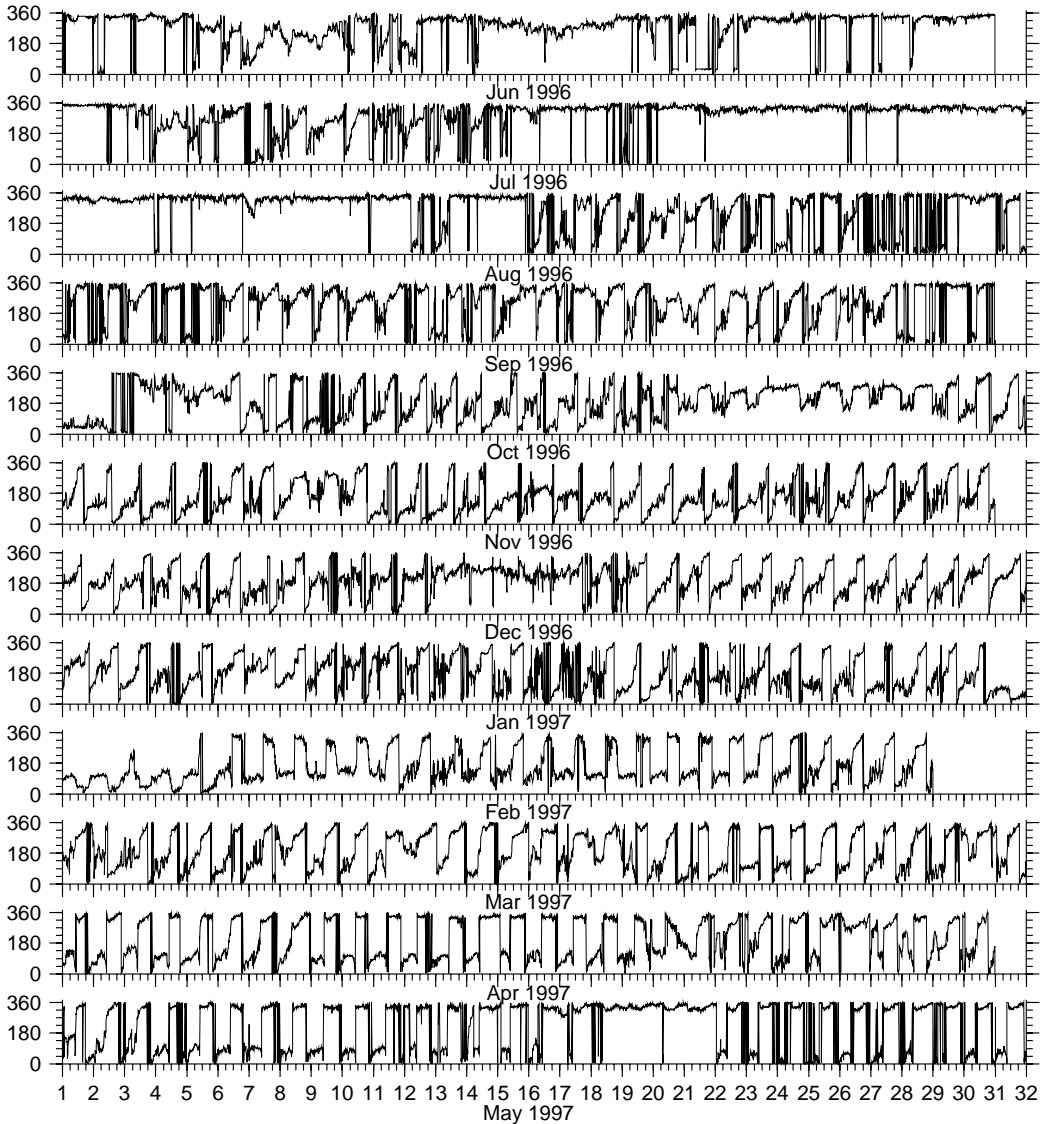


**Figure 1.14** Wind direction (in degrees clockwise from north; north is 0 degrees) from which the winds blew during 1 June 1996 to 31 May 1997. The horizontal axis gives date of the month shown at the bottom of each panel. Vertical axis gives direction.

hence sea-breeze circulation is expected to dominate coastal winds. In figure 1.15, wind vectors at 0600, 1200, 1800, and 0000 hours are identified. The wind speed usually picked up at 1000 hours (IST) and peaked around 1500 hours, the peak wind speed being about  $5 \text{ ms}^{-1}$ . By 2000h, the wind speed dropped to below  $3 \text{ ms}^{-1}$ , and decreased slowly thereafter. Minimal wind speed of about  $1.5 \text{ ms}^{-1}$  was observed at around 0600h. Before the onset of the sea breeze, the wind speed generally

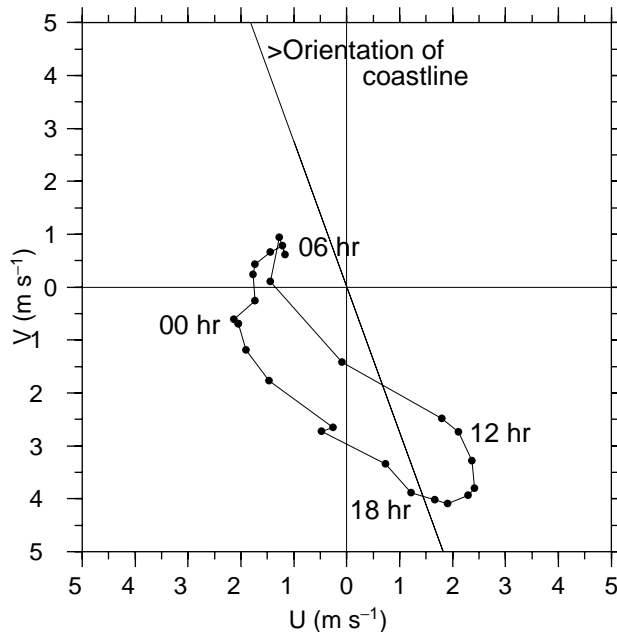


**Figure 1.15** Sea breeze hodograph for the average winds during 1–15 April 1997. The wind vectors at 0600, 1200, 1800, and 0000 hours are identified. Though there is day-to-day variation in the sea breeze (figure 1.13), on average, the sea breeze at about 1200 hours is approximately from the northwest. At this time, the wind has a component perpendicular to the coastline and is oriented towards the coast (see orientation of the coastline marked). By 1800 hours the wind vector turns towards the right, to a direction that is along the coast, and continues to turn further while the magnitude decreases.

remained less than  $2 \text{ m s}^{-1}$ . The onset was marked by an abrupt change in wind direction: before 1000 hours, the wind was from about  $90^\circ$ , but after onset, the direction changed to about  $300^\circ$  (figure 1.14). During 1000–2000 hours, the wind direction changed slowly from  $300^\circ$  to about  $360^\circ$ . The coastline in the vicinity of Goa is oriented along approximately  $340^\circ$ . Hence, the sea breeze recorded by the anemometer at a height of about 50 m above sea level is almost along the coastline. At sea level, the breeze is expected to be at an angle somewhat lower than the angle at the height of the anemometer owing to veering due to frictional effects in the atmospheric boundary layer.

Sea breeze is a common mesoscale meteorological phenomenon in many coastal areas of the world, including the area along the coastline of the Indian subcontinent. The effect of the phenomenon is felt over both land and sea. Aparna *et al.* (2005), quoting earlier studies, noted that the landward extent along the Indian coast is 110–150 km. They estimated that the sea breeze extends up to a distance of about 180 km off Goa. This inference was made using an objective method based on offshore decay of vector correlation.

## 1.5 WAVES

Concomitant with the wind observations during June 1996 to May 1997, waves were measured off the mouths of the Mandovi and Zuari estuaries using a Datawell directional waverider buoy in 23m of water. The instrument recorded 20-minute averaged wave spectra once every three hours. The most striking feature of the annual march of the spectra is the dramatically high wave energy observed during the summer monsoon when compared to the rest of the year. As seen in figure 1.16,

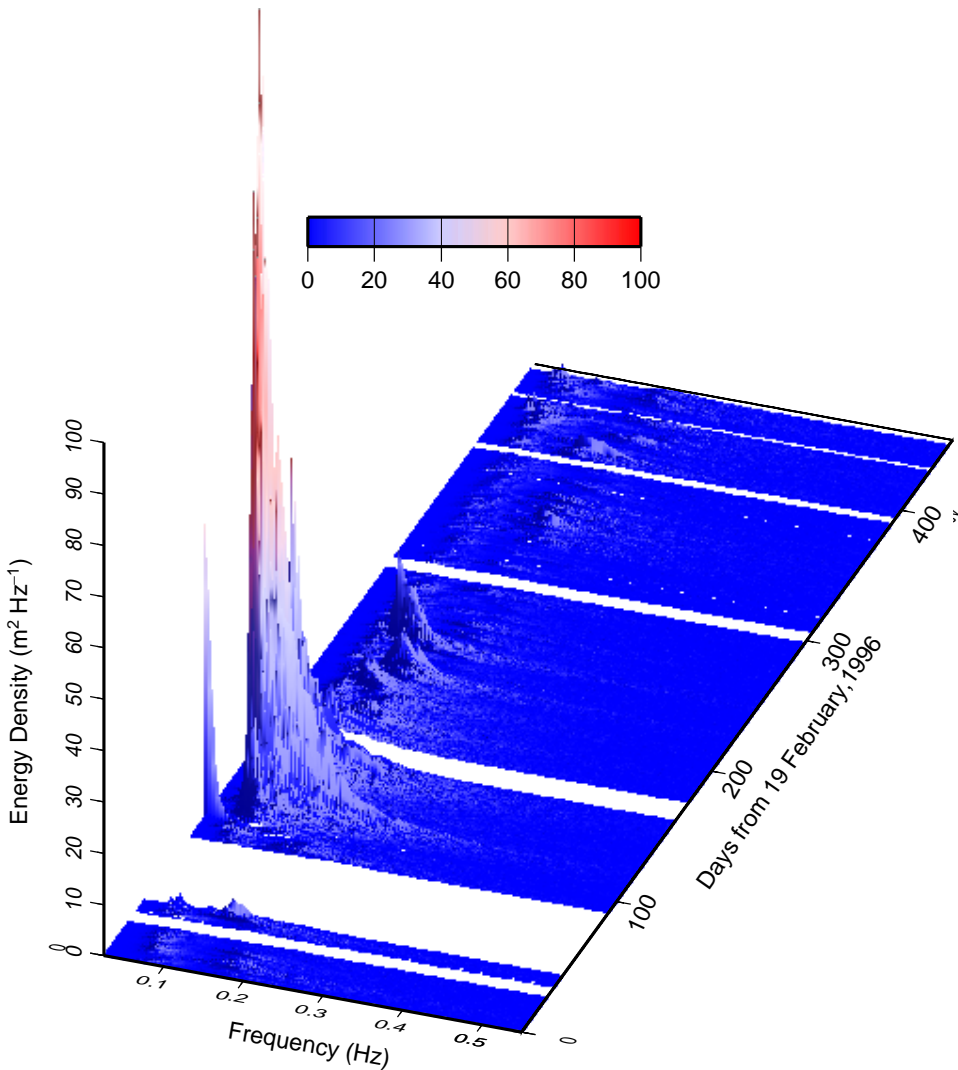


**Figure 1.16** Spectral density ( $\text{m}^2 \text{Hz}^{-1}$ ) as a function of frequency (Hz) at 3-hour interval during June 1996 to May 1997. White bands indicate missing data. Notice that most of the energy is seen during the summer monsoon.

peak spectral energy during the summer monsoon is about an order of magnitude larger than that observed during the rest of the year. The wave spectrum at this time is dominated by the swells that are generated over the open sea by the strong winds of the summer monsoon.

The energy of the swells reduces after the withdrawal of the monsoon. Soon, the sea breeze becomes an important feature of the winds in the coastal areas. Wave data show that the wave spectrum at this time often has two well-separated parts. The low-frequency part has energy with frequencies lesser than 0.15 Hz (i.e., periods longer than about 7 seconds) and represents the swells. The high-frequency part, or the “sea”, represents the spectrum of the locally generated waves. As seen in figure 1.17, which presents the evolution of the spectrum during 1–15 April 1997, the sea spectrum often shows diurnal variability. This is in contrast to the spectrum of

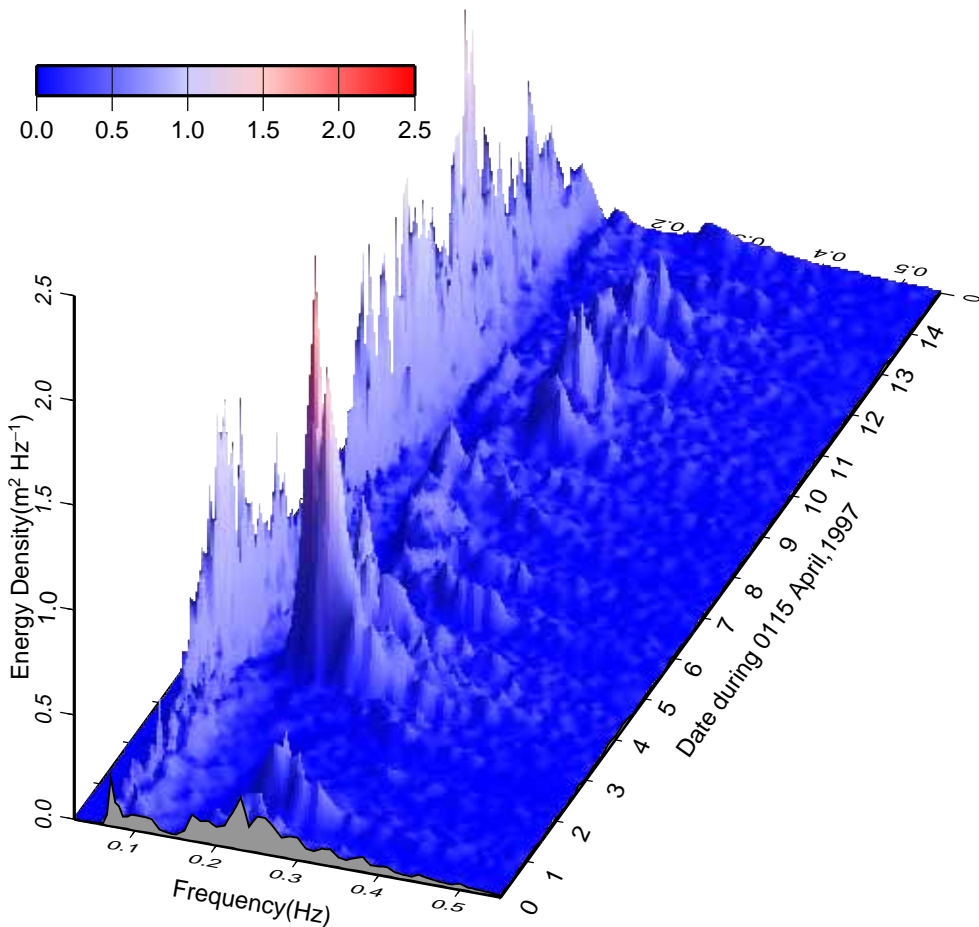


**Figure 1.17** Spectral density ( $\text{m}^2 \text{Hz}^{-1}$ ) as a function of frequency (Hz) at 3-hour interval during 1–15 April 1997.

swells. Neetu *et al.* (2006) have argued that the high-frequency spectrum is generated by the sea breeze on the continental shelf off Goa.

Wave spectra in shallow areas serve as good indicators of energy available for mixing of the water column. As seen above, the available energy is much larger during the summer monsoon than during the rest of the year. This is expected to have a major impact on vertical mixing near the mouths of the estuaries, in the Aguada Bay in the Mandovi and in the Mormugao Bay in the Zuari (see Map A). After withdrawal of the monsoon, the two bays have lesser energy coming into them from offshore, and the high-frequency part of this energy has a diurnal cycle. Contribution of energy from surface waves to vertical mixing in comparison to other available sources such as tidal stirring, is not known and needs to be explored, particularly in the two bays. It is expected that in the channels at the upstream ends of the two bays, the role of wind waves in vertical mixing would be significantly lower than that in the bays.

## 1.6 ESTUARINE REGIMES

As noted earlier, based on channel geometry, it is appropriate to divide each estuary into two parts: the bay and the channel. The former is wide, thus making along-estuary and cross-estuary physical processes similar in magnitude and importance. In the latter, along-estuary processes are by far the more important for temporal evolution of the estuary. The annual cycle of processes in each of these parts can be divided into two phases: wet and dry. The wet phase is about 4–5 months long and is characterized by high influx of freshwater. The dry phase is 7–8 months long and the influx of freshwater is either marginal or negligible. We can therefore divide the evolution of the annual cycle of the estuary into the four regimes depicted in figure 1.18. In the two-part name of each regime, the first part distinguishes the regime with respect to runoff, and the second part with respect to geometry. The four regimes are:

- ‘Wet-Bay’: This regime represents the bay in each estuary when freshwater influx into the bay is high, i.e., during the summer monsoon. When the influx is particularly high, such as when the monsoon is in an active phase, the bay turns into an almost entirely freshwater body. During lulls in the monsoon, tidal exchange across the wide mouth of the bay is expected to ensure that conditions similar to those on the shelf off the bay would also exist in the bay. This is one of the two regimes when mixing due to the influence of winds and waves is expected to be important. This regime is one of rapid temporal change in physical processes, and biogeochemical activity must adjust to this rapid change.
- ‘Wet-Channel’: This regime represents the channel in each estuary during the high runoff time of the summer monsoon. The channel at this time is primarily a freshwater body, except perhaps in the immediate vicinity of its bay-end. This



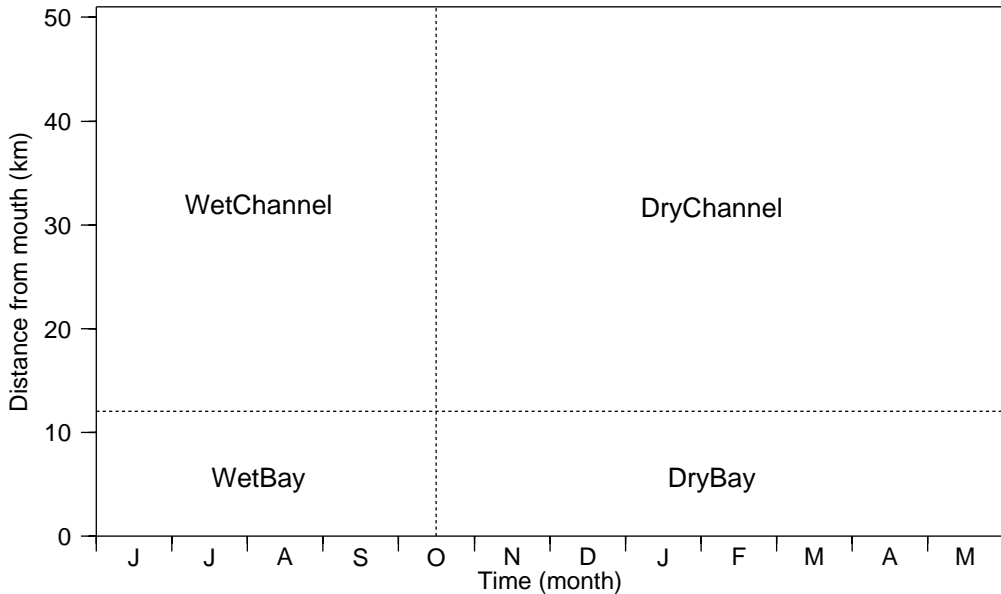


**Figure 1.18** Schematic of the four regimes into which the Mandovi and Zuari estuaries can be divided. See section 1.6 for details.

is the time of flushing of the estuary a few times over during the season. Each flushing renews the water in the channel completely.

- 'Dry-Bay': This regime represents the bay during the dry season. Tides are expected to make conditions in the bay similar to those that exist on the shelf offshore. This period of about 8 months is the time of temporal evolutions that is much slower than that seen during the 'Wet-Bay' regime. Winds, including the afternoon sea-breeze, are expected to contribute to vertical mixing in this regime.
- 'Dry-Channel': This is the most interesting of the four regimes. It is observed in the channels during about 7–8 dry months after the withdrawal of the monsoon. The regime is dominated by physical processes that ensure continuous intrusion of salt from the bay-end of the channel towards the head. Tides play an important role in the intrusion. The salt intrudes into the pool of freshwater created by the last episode of flushing during the summer monsoon. Of course, there is contribution of freshwater to the pool from runoff after the withdrawal of the monsoon. This contribution is expected to be small, but we do not have reliable estimates of it.

The four regimes define the state of each of the estuaries based on factors that are different from the internal working of the estuary. These regimes set the stage to put into perspective the internal working that forms the central theme of this book.

# References

---

- Achuthankutty C. T., Ramaiah N. and Padmavati G. (1997) Zooplankton variability and copepod assemblage in the coastal and estuarine waters of Goa along the central west coast of India; Intergovernmental Oceanographic Commission, 1 workshop report no. 142 (eds Pierrot-Bults A. C. and Vander Spoel S., UNESCO, Paris, pp 1–11.
- Alongi D. (1990) The ecology of tropical soft-bottom benthic ecosystems; *Oceanography and Marine Biology: An Annual Review* **28** 381–496.
- Álvares Claude (2002) Fish, Curry and Rice (Revised 4<sup>th</sup> edn.). Goa Foundation.
- Alzieu C. (2000) Environmental impact of TBT: the French experience; *Science of the Total Environment* **258** 99–102.
- Alzieu C. (2006) Effects of tributyltin pollution on oyster industry: the Arcachon Bay case; In: *Multiple dimensions of global environmental change* (ed.) Sangeeta Sonak, TERI Press, New Delhi, pp 444–458.
- American Society for Microbiology (1957) Manual of Microbiological Methods; ASM Press, Washington DC.
- Anonymous (2002) Guidance notes to the European Blue Flag Beach Criteria; 29p.
- Ansari Z. A., Ingole B. S. and Parulekar A. H. (1986) Spatial and temporal changes in benthic macrofauna from Mandovi and Zuari estuaries of Goa, west coast of India; *Indian Journal of Marine Sciences* **15** 223–229.
- Ansari Z. A., Ingole B. S. and Furtado R. (2003) Response of benthic fauna to different pollutants: Some case studies and relevance of benthos to environmental impact assessment; In: *Recent advances in environmental sciences* (ed.) Hiremath K. G. (Discovery Publishing House) pp 422–428.

- Aparna M., Shetye S. R., Shankar D., Shenoi S. S. C., Mehra P. and Desai R. G. P. (2005) Estimating the seaward extent of sea breeze from QuickSCAT scatterometry; *Geophysical Research Letters* **32** doi:10.1029/2005GL023107.
- Azam F. T., Fenchel J. G., Field J. S., Gray L. A., Mayer R. and Thingstad F. (1983) The ecological role of water column microbes in the Sea; *Marine Ecology Progress Series* **10** 257–263.
- Bhosle N. B. (2006) Butyltin compounds in biofilms and marine organisms from Dona Paula Bay west coast of India; In: *Multiple dimensions of global environmental change* (ed.) Sangeeta Sonak (New Delhi, TERI Press) pp 432–443.
- Brock T., Madigan M. T., Martinko J. M. and Parker J. (1994) *Biology of Microorganisms* (7<sup>th</sup> edn.). Prentice Hall, New Jersey.
- Bruland K. W., Franks, Knauer G. A. and Martin J. H. (1979) Sampling and analytical methods for the determination of copper, cadmium, zinc and nickel at nanogram per liter level in seawater; *Analytica Chimica Acta* **105** 233–245.
- Bhattathiri R. M. S., Devassy V. P. and Bhargava R. M. (1976) Production at different trophic levels in the estuarine system of Goa; *Indian Journal of Marine Sciences* **5** 83–86.
- Coe M. T. (2000) Modeling terrestrial hydrological systems at the continental scale: Testing the accuracy of an atmospheric GCM; *Journal of Climate* **13** 686–704.
- Costa, Cosme Jose (undated) Goa and her khajans. Instituto Menezes Braganca.
- Danielsson L.-G. (1980) Cadmium, cobalt, copper, iron, lead, nickel and zinc in Indian ocean waters; *Marine Chemistry* **8** 199–225.
- Dauer D. M. and Conner W. G. (1980) Effect of moderate sewage input on benthic polychaete populations; *Estuarine and Coastal Marine Science* **10** 335–362.
- de Sousa S. N. (1983) Studies on the behaviour of nutrients in the Mandovi estuary during premonsoon; *Estuarine, Coastal and Shelf Science* **16** 299–308.
- Dehadrai P. V. and Bhargava R. M. S. (1972) Seasonal organic production in relation to environmental features in Mandovi and Zuari estuaries, Goa; *Indian Journal of Marine Sciences* **1** 52–56.
- Devassy V. P. (1983) Plankton production associated with cold water incursion into the estuarine environment; *Mahasagar* **16** 221–233.
- Devassy V. P. and Goes J. I. (1988) Phytoplankton community structure and succession in a tropical estuarine complex (central west coast of India); *Estuarine, Coastal and Shelf Science* **27** 671–685.
- Devassy V. P. and Goes J. I. (1989) Seasonal patterns of phytoplankton biomass and productivity in a tropical estuarine complex (west coast of India); *Proceedings of the Indian Academy of Sciences (Plant Sciences)* **99** 485–501.

- Dufour A. P. (1984) Bacterial indicators of recreational water quality; *Canadian Journal of Public Health* **75** 49–56.
- ETOPO2 (2007) Online documentation. <http://www.ngdc.noaa.gov/mgg/fliers/06mgg01.html>.
- Friedrichs C. T. and Aubrey D. G. (1994) Tidal propagation in strongly convergent channels; *Journal of Geophysical Research* **99** 3321–3336.
- Fujioka R. (2002) Microbial indicators of marine recreational water quality; In: *Manual of Environmental Microbiology*, 2<sup>nd</sup> edn. (eds) Hurst C. J., Crawford R. L., Knudsen G., McIneney M. J. and Stetzenbach L. D., American Society for Microbiology Press, Washington DC, pp 234–243.
- Gauns M. (2000) Role of microzooplankton in the food chain dynamics of some tropical marine environments; Ph. D. Thesis, Goa University, India, pp. 220.
- Gerlach S. A. (1978) Food chain relationship in subtidal silty sand marine sediment and the role of meiofauna in stimulating bacterial productivity; *Oecologia* **33** 55–69.
- Geyer W. R., Townbridge J. H. and Bowen M. M. (2000) The Dynamics of a Partially Mixed Estuary; *Journal of Physical Oceanography* **30** 2035–2048.
- GLOBE (2004) The Global Land One kilometer Base Elevation (GLOBE) Digital Elevation Model. Version 1. 0. National Oceanic and Atmospheric Administration, National Geophysical Data Center, <http://www.ngdc.noaa.gov/mgg/topo/globe.html>.
- Godhantaraman N. (1994) Species composition and abundance of tintinnids and copepods in the Pichavaram mangroves (South India); *Ciencias Marinas* **20** 371–391.
- Goswami S. C. (1983) Coexistence and succession of copepod species in the Mandovi and Zuari estuaries, Goa; *Mahasagar* **16** 251–258.
- Government of Goa (1976) Goa, Daman and Diu Agricultural Tenancy Act, Fifth Amendment (GDD 17 of 1976, S3). Government Gazette (Extraordinary) No. 29, dated 14/10/1976.
- Grasshoff K., Ehrhardt M. and Kremling K. (1983) *Methods of Seawater Analysis*. Verlag Chemie, New York, NY, 419 pp.
- Harleman D. R. F. and Lee C. H. (1969) The computation of tides and currents in estuaries and canals; *Technical bulletin 16, M. I. T., Massachusetts*, 264 pp.
- Hoch M. (2001) Organotin compounds in the environment – an overview; *Appl. Organometallic Chemistry* **16** 719–743.
- Hwang H. M., Oh J. R., Kahng S. H. and Lee K. W. (1999) Tributyltin compounds in mussels, oysters, and sediments of Chinhae Bay Korea; *Marine Environmental Research* **47** 61–70.
- Jay D. A. and Musiak J. M. (1994) Particle trapping in estuarine tidal flows; *Journal of Geophysical Research* **99** 445–461.

- Jay D. A. and Musiak J. M. (1996) Internal tidal asymmetry in channel flows: Origins and consequences; In: *Mixing Processes in Estuarine and Coastal Seas* (ed.) Pattiaratchi C., AGU, Washington D. C., pp 211–249.
- Jay D. A. and Smith J. D. (1990) Residual circulation in shallow estuaries, 2, Weakly stratified and partially mixed estuaries; *Journal of Geophysical Research* **95** 733–748.
- JGOFS (1994) Protocols for the Joint Global Ocean Flux Study (JGOFS) core measurements, Manual and guides 29, Scientific Committee on Oceanic Research, United Nations Educational, Scientific and Cultural Organization, Paris, 170 pp.
- Jyothibabu R., Madhu N. V., Jayalakshmi K. V., Balachandran K. K., Shiyas C. A., Martin G. D. and Nair K. K. C. (2006) Impact of fresh water influx on microzooplankton mediated food web in a tropical estuary (Cochin backwaters), India; *Estuarine, Coastal and Shelf Science* **69** 505–515.
- Krishnakumari L., Bhattathiri P. M. A., Matondkar S. G. P. and John J. (2002) Primary productivity in Mandovi–Zuari estuaries in Goa; *Journal of the Marine Biological Association of India* **44** 1–13.
- Kristensen E. M., Jensen M. H. and Anderson T. K. (1985) The impact of polychaete (*Nereis virens* Sars) burrows on nitrification and nitrate reduction in sediments; *Journal of Experimental Marine Biology and Ecology* **85** 75–91.
- Leendertse J. J. and Gritton E. C. (1971) A water quality simulation model for well mixed estuaries; Vol. II, computation procedure; *R-708-NYC, The New York City Rand Institute technical report*, 53 p.
- Madhu N. V., Jyothibabu R., Balachandran K. K., Honey U. K., Martin G. D., Vijay J. G., Shiyas C. A., Gupta G. V. M. and Achuthankutty C. T (2007) Monsoonal variability in planktonic standing stock and abundance in a tropical estuary (Cochin Backwaters – India); *Estuarine, Coastal and Shelf Science* **3** 54–64.
- Madhupratap M. (1987) Status and strategy of zooplankton of tropical Indian estuaries: a review; *Bulletin of Plankton Society of Japan* **34** 65–81.
- Manoj N. T. and Unnikrishnan A. S. (2007) Tidal circulation and salinity distribution in Mandovi–Zuari estuaries; A numerical model study (unpublished manuscript).
- Mascarenhas A. and Chauhan O. S. (1998) A note on ancient mangroves of Goa, central west coast of India; *Indian Journal of Marine Sciences* **27** 473–476.
- McIntyre A. D. (1977) Effect of pollution on inshore benthos; In: *Ecology of marine benthos* (ed.) Coull B. C. (University of South Carolina Press) pp. 301–312.
- Miller C. B. (1983) The zooplankton of estuaries; In: *Estuaries and enclosed seas* (ed.) Ketchum B. H. (Amsterdam: Elsevier Scientific Publishing Company) pp. 103–149.
- Miranda de L. B., Castro de B. M. and Kjerfve B. (1998) Circulation and Mixing Due to Tidal Forcing in the Bertiooga Channel, Sao Paolo, Brazil; *Estuaries* **21** 204–214.

- Nair R. R., Hashimi N. H. and Gupta M. V. S. (1979) Holocene limestones of part of the western continental shelf of India; *Journal of Geological Society of India* **20** 17–23.
- Naqvi S. W. A, Naik H., Jayakumar D. A., Shailaja M. S. and Narvekar P. V. (2006) Seasonal oxygen deficiency over the western continental shelf of India; In: *Past and Present water column anoxia* (ed.) Neretin L. N., NATO Sci. Ser. IV: *Earth and Environmental Science* **64**, Dordrecht, The Netherlands: Springer, 195–224.
- Nayak R. K. and Shetye S. R. (2003) Tides in the Gulf of Khambhat, west coast of India; *Estuarine, Coastal and Shelf Science* **57** 249–254.
- Neetu S., Shetye S. R. and Chandramohan P. (2006) Impact of sea breeze on the wind-seas off Goa, west coast of India; *Journal of Earth System Science* **115** 229–234.
- Officer C. B. (1976) Physical oceanography of estuaries (and associated coastal waters); (New York: John Wiley & Sons) 465 p.
- Padmavati G. and Goswami S. C. (1996) Zooplankton ecology in the Mandovi–Zuari estuarine system of Goa, west coast of India; *Indian Journal of Marine Sciences* **25** 268–273.
- Panikkar N. K. (1969) New perspectives in estuarine biology; Proc. all India Symp. in Estuarine Biology, Madras, 27–30 December, 8 pp.
- Parulekar A. H., Dhargalkar V. K. and Singbal S. Y. S. (1980) Benthic studies in Goa estuaries. 3. Annual cycle of Macrofaunal distribution, production and trophic relation; *Indian Journal of Marine Sciences* **9** 189–200.
- Parulekar A. H. and Dwivedi S. N. (1973) Ecology of benthic production during southwest monsoon in an estuarine complex of Goa. Recent Researches in Estuarine Biology. (ed.) Natarajan R. (Delhi: Hindustan Publ. Co.) pp 21–30.
- Parulekar A. H., Harkantra S. N. and Ansari Z. A. (1982) Benthic production and assessment of demersal fishery resources of the Indian seas; *Indian Journal of Marine Sciences* **11** 107–114.
- Qasim S. Z. (1977) Biological productivity of the Indian Ocean; *Indian Journal of Marine Sciences* **6** 122–137.
- Qasim S. Z. and Sengupta R. (1981) Environmental characteristics of the Mandovi–Zuari estuarine system in Goa; *Estuarine, Coastal and Shelf Science* **13** 557–578.
- Qasim S. Z. (2003) Indian Estuaries. Allied Publishers, 420 pp.
- Rainer S. (1981) Temporal pattern in the structure of Macrobenthic communities of an Australian estuary; *Estuarine and Coastal Marine Science* **13** 597–619.
- Rao T. S. S. (1976a) Salinity and distribution of brackish warm water zooplankton in India estuaries; Proceedings of the Symposium on warm water zooplankton, 196–204.

- Rao V. P., Montaggioni L., Vora K. H., Almeida F., Rao K. M. and Rajagopalan G. (2003) Significance of relic carbonate deposits along the central and southwestern margin of India for late Quaternary environmental and sea level changes; *Sedimentary Geology* **159** 95–111.
- Rao Y. P. (1976b) Southwest Monsoon; *India Meteorological Monograph (Synoptic Meteorology)*, No. 1/1976, Delhi, 376 pp.
- Robertson J. R. (1983) Predation by estuarine zooplankton on tintinnid ciliates; *Estuarine, Coastal and Shelf Science* **25** 581–591.
- Rubinoff J. A. (2001) Pink Gold: Transformation of backwater aquaculture on Goa's Khazan Lands; *Economic & Political Weekly*, 36:13, pp. 1108–1114. Memorial Library Periodical: AP E19 A543.
- Samant D. (2006) Abundance of pollution indicator and certain human pathogenic bacteria in Mandovi–Zuari estuaries; M. Sc. Thesis. University of Goa, 63p.
- Sankaranarayanan V. N. and Qasim S. Z. (1969) Nutrients of the Cochin backwaters in relation to environmental characteristics; *Marine Biology* **2** 236–247.
- Shankar D., Kotamraju V. and Shetye S. R. (2004) A quantitative framework for estimating water resources in India; *Current Science* **86** 543–552.
- Shetye S. R., Gouveia A. D., Shenoi S. S. C., Sundar D., Michael G. S., Almeida A. M. and Santanam K. (1990) Hydrography and circulation off the west coast of India during the southwest monsoon 1987; *Journal of Marine Research* **48** 359–378.
- Shetye S. R., Gouveia A. D., Singbal S. Y., Naik C. G., Sundar D., Michael G. S. and Nampoothiri G. (1995) Propagation of tides in the Mandovi–Zuari estuarine network; *Proceedings of the Indian Academy of Sciences (Earth and Planetary Sciences)* **104** 667–682.
- Shetye S. R. and Murty C. S. (1987) Seasonal variation of salinity in the Zuari estuary, Goa, India; *Proceedings of the Indian Academy of Sciences (Earth and Planetary Sciences)* **96** 249–257.
- Shetye S. R., Shenoi S. S. C., Antony M. K. and Krishnakumar V. (1985) Monthly mean wind stress along the coast of the north Indian Ocean; *Proceedings of the Indian Academy of Sciences (Earth and Planetary Sciences)* **94** 129–137.
- Simpson J. H., Brown J. Matthews J. and Allen G. (1990) Tidal Straining, Density Currents, and Stirring in the Control of Estuarine Stratification; *Estuaries* **13** 125–132.
- Sonak S., Kazi S. and Abraham M. (2005) Khazans in troubled waters (TERI Press, The Energy Research Institute, New Delhi).
- Stacey M. T., Bura J. R. and Monismith S. G. (2001) Creation of residual flows in a partially stratified estuary; *Journal of Geophysical Research* **106** 17,013–17,037.

- Stoecker D. K. and Capuzzo J. M. (1990) Predation on protozoa: its importance to zooplankton; *Journal of Plankton Research* **12** 891–908.
- Sundar D. and Shetye S. R. (2005) Tides in the Mandovi and Zuari estuaries, Goa, west coast of India; *Journal of Earth System Science* **114** 493–503.
- Suprit K. and Shankar D. (2007) Resolving orographic rainfall on the Indian west coast; *International Journal of Climatology*, in press.
- Suresh I. and Shetye S. R. (2007) An analytical model for the propagation of tides in the Mandovi and Zuari estuaries, Goa, west coast of India (unpublished manuscript).
- Tamaki A. and Ingole B. S. (1993) Distribution of juvenile and adult ghost shrimps, *Callinassa japonica* Ortmann (Thalassinidea), on an intertidal sandflat: Intraspecific facilitation as a possible pattern-generating factor; *Journal of Crustacean Biology* **13** 175–183.
- Tomas C. R. (1997) *Identifying Marine Phytoplankton* (New York: Academic Press) 858 pp.
- Townbridge J. H., Geyer W. R., Bowen M. M. and Williams A. J. III (1999) Near-bottom Turbulence Measurements in a Partially Mixed Estuary: Turbulent Energy Balance, Velocity Structure, and Along-Channel Momentum Balance; *Journal of Physical Oceanography* **29** 3056–3072.
- Unnikrishnan A. S., Shetye S. R. and Gouveia A. D. (1997) Tidal propagation in the Mandovi–Zuari estuarine network, west coast of India: Impact of freshwater influx; *Estuarine, Coastal and Shelf Science* **45** 737–744.
- Wadia D. N. (1975) *Geology of India* (4<sup>th</sup> edn.). Tata McGraw-Hill Publishing Company Limited, New Delhi.
- Wafar S. (1987) *Ecology of mangroves along the estuaries of Goa*; Ph. D. Thesis, Karnataka University, Dharward.
- Wafar S., Untawale A. G. and Wafar M. V. M. (1997) Litter fall and energy flux in a mangrove ecosystem; *Estuarine, Coastal and Shelf Science* **44** 111–124.
- Xavier, Filipe Neri (1852) *Bosquejo Historico das Comunidades das Aldeas dos Conselhos das Ilhas, Bardez e Salcete*. Part I Govt. of Goa, pp 90.